Bioorganic & Medicinal Chemistry Letters 22 (2012) 3732–3738

Contents lists available at SciVerse ScienceDirect

Bioorganic & Medicinal Chemistry Letters

journal homepage: www.elsevier.com/locate/bmcl

The design, synthesis, and biological evaluation of PIM kinase inhibitors

Amy Lew Tsuhako *, David S. Brown, Elena S. Koltun, Naing Aay, Arlyn Arcalas, Vicky Chan, Hongwang Du, Stefan Engst, Maurizio Franzini, Adam Galan, Ping Huang, Stuart Johnston, Brian Kane, Moon H. Kim, A. Douglas Laird, Rui Lin, Lillian Mock, Iris Ngan, Michael Pack, Gordon Stott, Thomas J. Stout, Peiwen Yu, Cristiana Zaharia, Wentao Zhang, Peiwen Zhou, John M. Nuss, Patrick C. Kearney, Wei Xu

Exelixis, Department of Drug Discovery, 210 East Grand, South San Francisco, CA 94080, USA

ARTICLE INFO

Article history:
Available online 11 April 2012

Keywords:
PIM-1
PIM-2
PIM-3
CK2 inhibitor
Cdc7 inhibitor
Benzofuropyrimidinone

ABSTRACT

A series of substituted benzofuropyrimidinones with pan-PIM activities and excellent selectivity against a panel of diverse kinases is described. Initial exploration identified aryl benzofuropyrimidinones that were potent, but had cell permeability limitation. Using X-ray crystal structures of the bound PIM-1 complexes with **3**, **5m**, and **6d**, we were able to guide the SAR and identify the alkyl benzofuropyrimidinone (**6l**) with good PIM potencies, permeability, and oral exposure.

Proviral integration site of moloney murine leukemia virus (PIM) is a constitutively active serine/threonine protein kinase whose family consists of three highly related proteins, PIM-1, 2, and 3.[1,2] Since PIM kinases do not need prior post-translational modifications for the induction of kinase activity, they are tightly regulated at the transcriptional and translational level by cytokines, mitogens, and growth factors in the JAK/STAT pathway.[3] PIM's role in the cell is to suppress apoptosis through the direct phosphorylation of BCL-2 associated agonist of cell death (BAD).[4] Aside from its role in regulating cell survival, overexpression of PIM's has been reported in select solid tumors and many hematologic cancers such as chronic lymphocytic leukemia, Flt3-mediated acute myelogenous leukemia and diffuse B cell lymphoma.[5–8] These evidence strongly suggest PIM as an interesting target for cancer therapy.

Several groups have reported PIM inhibitors in the literature.[9–23] PIM-2 has been intrinsically more difficult to target primarily due to its high K_m for ATP.[17] Our efforts towards designing a pan-PIM inhibitor began with a high throughput screen (HTS) of our internal small molecule library against PIM-1 and PIM-2. These screens led to the discovery of benzofuropyrimidinone **1** (Fig. 1). While **1** was only moderately potent against PIM (PIM-1: IC_{50} = 526 nM, PIM-2: IC_{50} = 2963 nM, PIM-3: IC_{50} = 346 nM), this compound showed structural similarities to uncyclized **2**, a pyrimidinone that was identified from our internal CK2 inhibitor program, but showed cross reactivity with PIM (PIM-1: IC_{50} = 75 nM, CK2: IC_{50} = 32 nM). Synthesis of an analog that hybridized **1** and **2**, by incorporating a 2-chloro phenyl group to HTS hit **1**, gave compound **3**, an analog with significantly improved PIM-1 and PIM-3 activities and modest selectivity over CK2 (Fig. 1).

ATP competition studies found **3** to be an ATP competitive inhibitor. Furthermore, co-crystallization of **3** with PIM-1 revealed that while **3** binds in the ATP binding pocket, unlike typical kinase inhibitors that bind in this region, there are no hydrogen bond interactions with the hinge. This is a unique feature of PIM inhibitors as the hinge sequence of PIM has a proline insertion such that the hinge region bulges away from the ATP-binding site by up to 4 Å.[24–26] Consequently, the primary interactions for **3** that derive

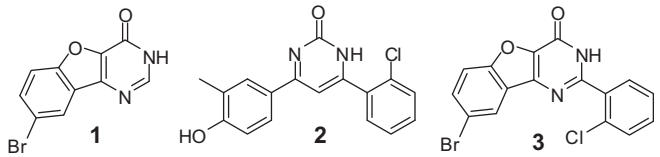

Figure 1. Early PIM leads.

* Corresponding author. Tel.: +1 6508378042.
E-mail addresses: alew@exelixis.com, amy.lew@gmail.com (A.L. Tsuhako).

0960-894X/$ - see front matter © 2012 Elsevier Ltd. All rights reserved.
http://dx.doi.org/10.1016/j.bmcl.2012.04.025

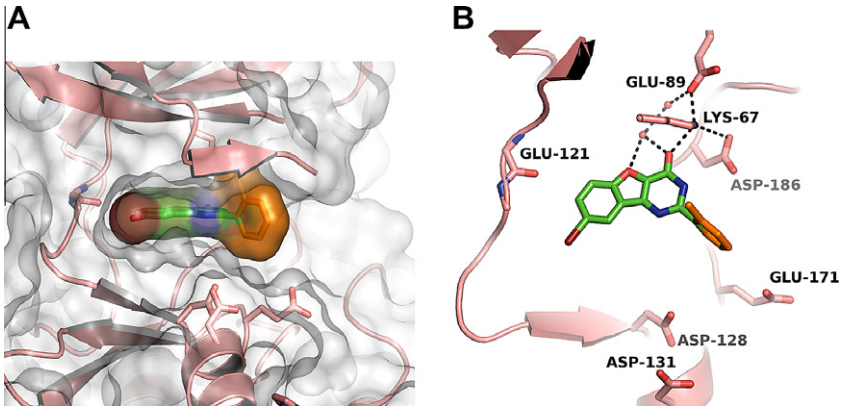

Figure 2. (A) CPK view of the crystal structure of **3** in PIM-1 solved to 2.6 Å showing the close packing of the bromide against the hinge (PDB code 4ALU). (B) Compound **3** crystallized in PIM-1 (Pink). The 2-Cl phenyl is disordered (Orange atoms indicate non-resolved disorder).

Table 1
Biochemical inhibitory activity for left hand modifications

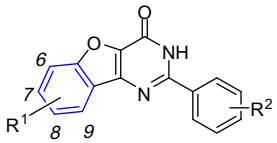

ID	R_1	R_2	Kinase inhibitory activity IC_{50}[a] (nM)			
			PIM-1	PIM-2	PIM-3	CK2
3	8-Br	2-Cl	17	781	18	231
4a	H	2-Cl	5000	5000	5000	5000
4b	8-Cl	2-Cl	28	858	30	371
4c	8-Me	2-Cl	99	3934	104	2625
4d	8-OMe	2-Cl	61	1451	31	312
4e	8-OH	2-Cl	232	3755	106	1288
4f	8-CN	2-Cl	281	3429	204	5000
4g	8-Ph	2-Cl	3963	5000	88	5000
4h	8-OCF3	2-Cl	293	5000	286	5000
4i	8-CF3	2-Cl	23	2330	102	5000
4j	8-NH2	2-Cl	5000	5000	4393	5000
4k	8-NHMe	2-Cl	2982	5000	1244	5000
4l	8-NHAc	2-Cl	5000	5000	1168	5000
4m	7-OH	2-Cl	205	2377	71	2485
4n	7-OMe	2-Cl	5000	5000	5000	5000
4o	9-OMe	2-Cl	1871	5000	850	3471
4p		2-Cl, 6-F	497	3330	166	3457

[a] Values reported are the average of at least two independent dose–response curves; variation was generally 15%.[29,30]

PIM potency are from van der Waals interactions of the 8-bromo benzofuropyrimidinone core with the linker region, a potential π stacking between the 2-chloro phenyl and Phe49, and a salt bridge that forms between the pyrimidinone C=O and Lys67 (Fig. 2).

To optimize the potency of **3** for PIM over CK2, we first looked towards modifying the left-hand side (Table 1). We found that the 8-Br was necessary for activity, as the des-Br analog **4a** was inactive. Replacement of the 8-Br with 8-Cl was tolerated (**4b**), but replacement with larger functionalities such as a cyano or phenyl were not (**4f**, **4g**). This was expected, as the crystal structure of **3** in PIM-1 showed that the 8-Br was packed tightly against the hinge region (Fig. 2A). Interestingly, the 8-CF_3 analog was more potent against PIM-1 than the non-halogenated 8-Me analog **4c**, indicating that a dipole interaction between the ligand and protein was important in this region. However, this dipole is very directed as 8-OCF_3 (**4h**) was less potent than 8-OMe (**4d**).

Aside from space constraints, there were also no hydrogen bonding opportunities in the 8-position as neither 8-OH, nor

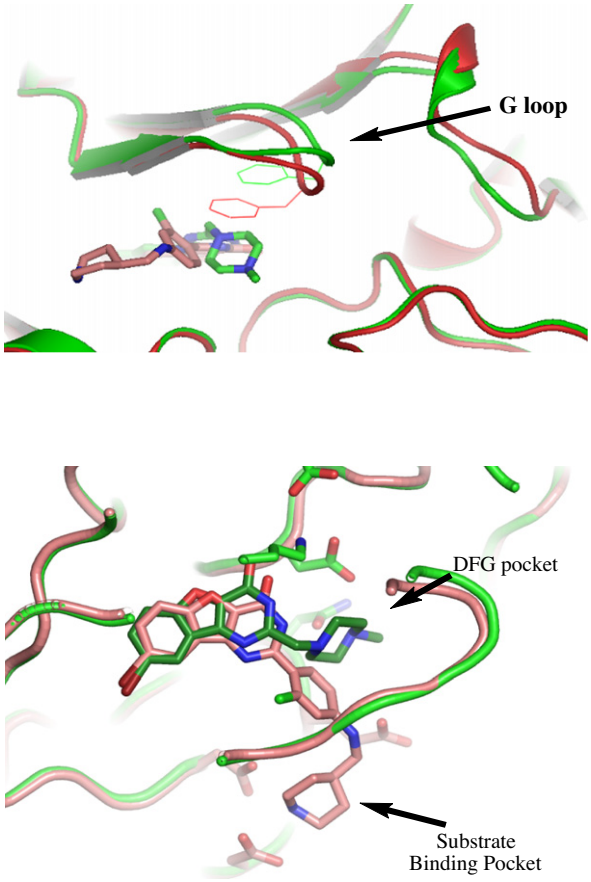

Figure 3. Comparison of aryl versus alkyl benzofuropyrimidinone binding modes in PIM-1. Compound **5m** co-crystallized with PIM-1 (PDB code 4ALV) is shown in pink (2.59 Å) and overlaid with compound **6d** co-crystallized in PIM-1 (PDB code 4ALW) shown in green (1.92 Å). (A) Side view showing the opening of the G-loop. (B) Front view showing the aryl piperidine group on **5m** pointing in a different direction from that of the alkyl piperazine on **6d**.

8-NH_2 was more potent than lead compound **3**. However, the crystal structure of **3** in PIM-1 showed that the carbonyl backbone of Glu121 in the linker region was accessible for hydrogen bonding if a hydroxyl group was placed in the 7-position instead of 8-position of the benzofuropyrimidinone (Fig. 2B). Unfortunately, the 7-OH analog (**4m**) was less potent than lead compound **3**. Since the SAR on the left-hand side of the benzofuropyrimidinone **3** was

steep, we decided to switch our focus to optimizing the right-hand side while holding the left-hand side constant as the 8-Br.

Based on the X-ray crystal structure of **3**, the right-hand portion of the molecule appeared to leave more room for modification than the left-hand side (Fig. 2A). The 2-Cl phenyl group can favorably interact with the nearby Phe49; although the 2-Cl phenyl was disordered in both the PIM-1 (Fig. 2B) and CK2 crystal structures (data not shown). MS/MS and LC/MS analysis of **3**, and the protein complex with **3**, demonstrated that the 2-Cl phenyl group was intact (data not shown). Once the 2-Cl phenyl was substituted with larger functional groups (i.e., **5m**, Fig. 3), no disorder of this moiety was observed in PIM complex crystal structure.

Modification of the right-hand side began with surveying replacements for the 2-Cl functionality. Unfortunately, none of these replacements were fruitful. For example, 2-OMe and 2-*i*Pr phenyl were both inactive against PIM (Table 2, **5a** and **b**). On the other hand, di-substituted phenyl analogs with a 2-Cl group, maintained potency and selectivity for PIM-1 and PIM-3 (**5c**–**5h**). Especially noteworthy was **5f**, where the PIM-1 and PIM-3 potencies were below 10 nM, and CK2 activity was >10-fold of PIM activities. Despite having potencies in PIM-1 and PIM-3, **5f** did not have PIM-2 potency. Understandably, PIM-2 inhibition will be more difficult to attain due to the significant differences in affinity for ATP between these proteins. The K_m of ATP for PIM-1 is 343 μM at 1 mM of substrate, while the K_m of ATP for PIM-2 is 2.3 μM at the same substrate concentration.[27]

To further improve pan-PIM potency and selectivity, we looked towards molecular modeling studies. These modeling studies hinted that we could improve pan-PIM potency by designing analogs that could hydrogen bond with the three non-conserved acidic residues (Asp128, Asp 131, Glu171) in the PIM substrate binding pocket (Fig. 2B). A number of analogs with different 1°, 2° and 3° amines tethered via an aniline, amide or methylene off of the *para*-position of the 2-Cl phenyl were synthesized and representative examples are shown in Table 2 (**5j**–**5m**). Indeed, we found that these basic amines improved PIM-1, 2 and 3 activities, especially PIM-2 activities; but although these aryl benzofuropyrimidinones had biochemical potencies below 10 nM for PIM-1/-3, and below 100 nM for PIM-2, they were not potent in cells. Evaluation of this series of amine tethered benzofuropyrimidinone analogs in MDCK cells indicates permeability as an issue, presumably due to the higher molecular weight (487–530 amu), and high lipophilicity (*c*log*P* 4.9–5.2).

To improve the cell permeability, we wanted to replace the large right-hand di-substituted aryl groups with simpler alkyl amino groups that would still allow access to the three acidic residues in the substrate binding pocket, but might offer improved physicochemical properties. Initially, simple alkyl amines such as a piperidine, pyrrolidine, azetidine and methyl-piperazine tethered via a methylene group to the benzofuropyrimidinone core were synthesized (Table 3: **6a**–**6d**). We were encouraged to find that the alkyl amino benzofuropyrimidinones were as potent in PIM as the aryl

Table 2
Biochemical inhibitory activity for right hand modifications of the aryl ring

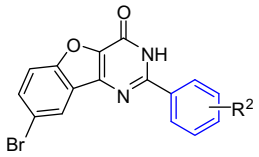

ID	R_2	Kinase inhibitory activity IC_{50}[a] (nM)				MDCK (nm/s)
		PIM-1	PIM-2	PIM-3	CK2	
3	2-Cl	17	781	18	231	—
5a	2-OMe	>5000	>5000	>5000	5000	—
5b	2-*i*Pr	376	5000	810	1419	—
5c	2-Cl, 4-F	24	850	23	243	289
5d	2-Cl, 5-F	14	653	13	173	42
5e	2-Cl, 6-F	35	1068	23	743	336
5f	2-Cl, 3-Cl	8	598	8	269	77
5g	2-Cl, 4-Cl	11	293	17	95	11
5h	2-Cl, 3-OMe	15	1741	21	575	197
5i	2-Cl, 4-CH_2NH_2	3	87	8	184	93
5j	2-Cl, 4- 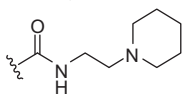	4	134	20	94	8
5k	2-Cl, 4- 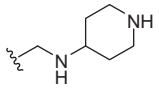	4	29	8	339	3
5l	2-Cl, 4- 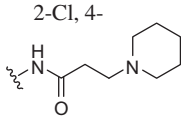	3	68	5	194	68
5m	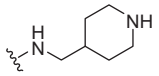	7	29	8	2122	4

[a] Values reported are the average of at least two independent dose–response curves; variation was generally 15%.[29,30]

Table 3
Biochemical inhibitory activity for right hand modifications with alkyl groups

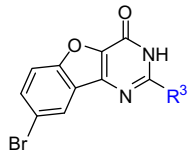

ID	R_3	Kinase inhibitory activity IC_{50}[a] (nM)				MDCK (nm/s)
		PIM-1	PIM-2	PIM-3	CK2	
6a	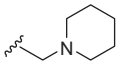	32	730	41	147	481
6b	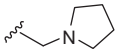	13	194	12	92	848
6c	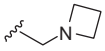	9	68	10	115	499
6d	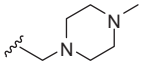	27	197	11	2950	475
6e	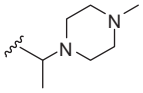	16	503	35	3151	461
6f	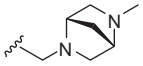	10	110	9	582	68
6g	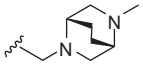	3	162	18	452	129
6h	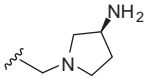	4	49	11	68	10
6i	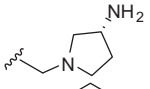	6	72	6	535	9
6j	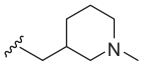	18	534	31	484	83
6k	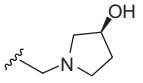	11	121	10	28	172
6l	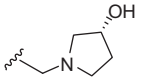	5	68	4	95	152
6m	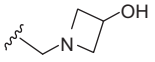	10	142	11	87	81

[a] Values reported are the average of at least two independent dose–response curves; variation was generally ±15%.[29,30]

benzofuropyrimidinones; and more importantly, showed improved cellular permeability. For example, azetidine analog **6c** showed pan-PIM activities with excellent MDCK value.

Interestingly, the crystal structure of PIM-1 with **6d** revealed that the alkyl benzofuropyrimidinones did not bind in the ATP pocket in the same manner as the aryl benzofuropyrimidinones (Fig. 3). Rather than the piperazine occupying the substrate binding pocket as predicted, the molecule is shifted closer to Lys67, and the piperazine forces the G-loop and Phe49 out, allowing the distal amine on the piperazine to make a hydrogen-bond contact with the Asp186 of the DFG loop. In fact, the presence of the distal amine and the hydrogen bonding capability with Asp186 is what drives this G-loop movement. We were encouraged by this finding as it showed that there was more room in the DFG pocket than originally thought.

Increasing the steric bulk around the piperazine to maximize van der Waals contact with the expanded DFG pocket resulted in analogs **6e**–**6g** that showed improved PIM-1 activities compared to the parent piperazine analog **6d**, but did not improve PIM-2 or 3 activities. Consequently, rather than maximizing van der Waals

Table 4
Biochemical inhibitory activity for left hand modifications in the alkyl benzofuropyrimidinone series

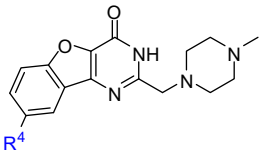

ID	R_4	Kinase inhibitory activity IC_{50}[a] (nM)			
		PIM-1	PIM-2	PIM-3	CK2
6d	Br	27	197	11	2950
7a	Cl	77	480	34	5000
7b	I	24	140	11	2800
7c		580	840	160	5000
7d		640	620	250	5000

[a] Values reported are the average of at least two independent dose–response curves; variation was generally 15%.[29,30]

Table 5
Cell potency, mouse and rat pk properties of compounds with pan-PIM activities

ID	Inhibition of phosphorylation in HEL 92.1.7 BAD S112 IC_{50}[a] (nM)	Mouse HTS PK dosed at 100 mg/kg (po) Plasma exposure (μM) 1h/4h	Rat PK						
			Dose (mg/kg)	CL (mL/h/kg)	V_d (L/kg)	$T_{1/2}$ (h)iv/po	F (%)	C_{max} (μM)iv/po	AUC/dose (μM h kg/mg)iv/po
6c	1051	13/5	2.5	1837	3.8	1.0/1.0	77	1.8/0.8	1.7/1.3
6f	2412	11/7	5	2044	7.1	2.6/2.6	86	1.5/0.4	1.2/0.9
6i	2582	6/5	5	3371	6.2	1.4/1.6	13	1.8/0.1	0.8/0.1
6l	1218	93/35	5	793	2.3	2.7/4.7	79	7.6/3.1	3.8/2.9
6m	1963	78/22	2.5	810	2.4	8.4/3.7	56	3.5/1.2	2.6/1.5

[a] IC_{50} values reported are the average of at least two independent dose–response curves.[31]

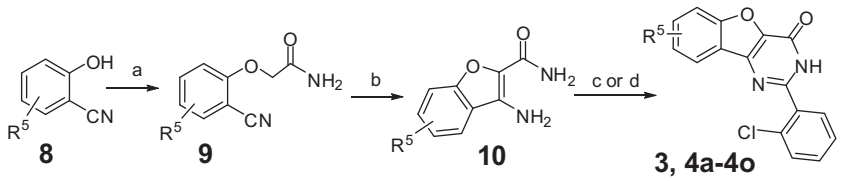

Scheme 1. Reagents and conditions: (a) Bromoacetamide, Cs_2CO_3, DMA, 75 °C; (b) KOH, EtOH, 75 °C; (c) 2-chloro-benzaldehyde, cat. concd HCl, 150 °C; (d) 2-chlorobenzaldehyde, $CuCl_2$, EtOH, 120 °C microwave, 20 min

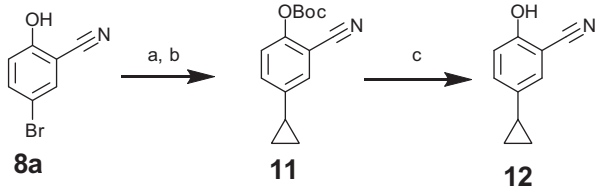

Scheme 2. Reagents and conditions: (a) Boc_2O, DMAP, DCM, ACN, 99% yield; (b) cyclopropyl boronic acid, $Pd(OAc)_2$, PCy_3, K_3PO_4, toluene, H_2O, 67% yield; (c) TFA, Et_3SiH, DCM.

contacts, we decided to optimize the hydrogen-bond contact with the Asp of the DFG pocket by installing an amino-pyrrolidine or installing a 3-piperidine (**6h**–**6j**). While this strategy gave pan-PIM active analogs **6h** and **6i**, the cell permeabilities were compromised due to the presence of primary amines. Replacement of the 1° amine with a hydroxyl (**6k**, **6l**) substantially improved the MDCK and cell potency while maintaining PIM activities (Tables 3 and 5).

Since the alkyl benzofuropyrimidinones bind in the ATP pocket differently from the aryl benzofuropyrimidinones, we wanted to go back and re-optimize the left-hand side 8-position to see if methylpiperazine derivatives leave more room for modifications. Unfortunately, even replacement of the 8-bromide with an 8-chloride which was previously tolerated in the aryl series (**4b**), was now significantly less potent in the alkyl series (**7a**). A larger halide such as the 8-iodo analog (**7b**) was equipotent to the 8-bromo analog, but a non-halide such as the 8-cyclopropyl (**7c**) was inactive, similar to what we had observed for the aryl series (**4p** vs **5e**).

Compounds with pan-PIM activities, and ⩾10-fold selectivity for CK2 with respect to both PIM-1 and PIM-3, were then evaluated in PK studies (Table 5). Compound **6l** showed high plasma exposures (1h/4h) in mouse high-throughput screening PK dosed at

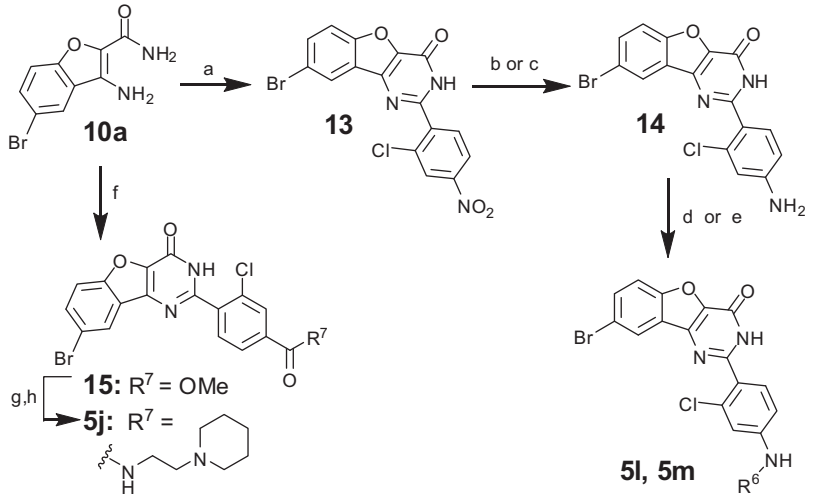

Scheme 3. Reagents and conditions: (a) 2-Chloro-4-nitrobenzaldehyde (2.3 equiv), $NaHSO_3$ (7 equiv), DMSO, 150 °C, 5 h; (b) sodium dithionite, THF/H_2O, rt 15 min; (c) $SnCl_2{\cdot}H_2O$, MeOH, EtOAc, H_2O, 80 °C, 1 h; (d) alkyl aldehyde, $NaBH(OAc)_3$, HOAc, DCE; (e) acid chloride, pyridine, DCM, rt; (f) methyl 3-chloro-4-formylbenzoate, $CuCl_2$, MeOH, 120 °C microwave, 20 min; (g) LiOH, 50 °C; (h) HATU, DIEA, DMF, various amines.

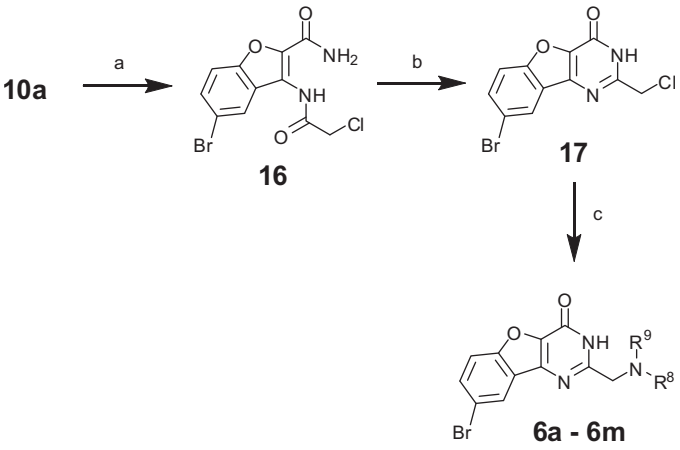

Scheme 4. Reagents and conditions: (a) Chloroacetyl chloride, 40 °C, 30 min, 90% yield; (b) 2 N NaOH, 40 °C, 20 min, 63% yield; (c) alkyl amine, EtOH, 80 °C.

100 mg/kg, and a favorable Rat PK profile with high bioavailability and good absorption. Selectivity profiling pointed out Cdc7 as the only other kinase that was significantly inhibited (IC_{50} activities were >3600 nM for a panel of 30 kinases including c-Kit, Flt-3, JAK2, PDGFR, and KDR). In addition, the cytochrome P450 profile for **6l** showed limited inhibition of the major isoforms: CYP3A4 (MDZ), 2C8, 2C9, 2C19, 2D6 IC_{50}'s >20 μM; CYP1A2 IC_{50} = 5.1 μM. In mechanistic cellular assays with HEL92.1.7 cells, **6l** caused a dose dependent inhibition of the phosphorylation of BAD at the PIM kinase specific site S112. This inhibitory effect in cells is believed to be due to PIM activity since **6l** is not biochemically active against JAK2 or Flt-3 (IC_{50} >3600 nM).

The compounds in Table 1 were synthesized according to Scheme 1 where an appropriately substituted hydroxybenzonitrile (**8**) was alkylated with bromoacetamide under mildly basic conditions at 75 °C to give the corresponding cyanophenoxy-acetamide **9**.[28] Heating of **9** under basic conditions induced cyclization to give aminobenzofuran-carboxamide **10**. Formation of the benzofuropyrimidinone required cyclization under high temperatures with 2-chlorobenzaldehyde and a catalytic amount of acid, either concentrated HCl or copper(II) chloride. Without the high temperatures, the reaction stopped at the 2,3-dihydrobenzofuropyrimidinone stage. Synthesis of the cyclopropyl analog **4p** (Scheme 2) required Boc protection of the phenol, followed by Suzuki coupling of the bromide with the corresponding cyclopropyl boronic acid to give **11**. Boc deprotection gave the corresponding phenol that was then used to synthesize **4p** and **7c**.

The compounds in Table 2 were synthesized according to Scheme 3 where instead of cyclization with 2-chlorobenzaldehyde, **10a** was cyclized with 2-chloro-4-nitrobenzaldehyde to give intermediate **13**. The nitro group was then reduced with sodium dithionite or tin(II) chloride to give aniline **14**, which was either acylated with a variety of acid chlorides, or reductively alkylated with a variety of aldehydes. The reverse amides in this table were made by reacting methyl-3-chloro-4-formylbenzoate with **10a** to give the corresponding benzofuropyrimidinone **15**. The methyl ester was then saponified and the corresponding acid was activated with HATU for couplings with amines.

The compounds in Table 3 were synthesized according Scheme 4 where intermediate **10a** was reacted with chloroacetyl chloride to give intermediate **16**. Cyclization under basic conditions occurs rapidly to give chloromethyl benzofuropyrimidinone **17**, which can then be displaced with a variety of alkyl amines. The compounds in Table 4 were also synthesized in an analogous manner where the starting hydroxy-bromobenzonitrile was substituted with the corresponding chloro, iodo or cyclopropyl hydroxybenzonitrile.

In summary, we describe a novel class of benzofuropyrimidinones for PIM kinase inhibition. Using structure based design, we were able to successfully optimize lead **3** from a PIM-1/-3 inhibitor to a pan-PIM inhibitor, **6l**, with cellular potency and good oral exposure. In addition, through the SAR, we discovered that the G-loop of PIM-1 was flexible, opening up the pocket for hydrogen bonding opportunities with the DFG motif.

Acknowledgments

We greatly appreciate the contributions to the biochemical and pharmacokinetic data from members of Exelixis Genome Biochemistry, New Lead Discovery, Pharmacology and Compound Repository. In addition, we greatly appreciate Jia Li for additional PIM-1 co-crystals not reported in this manuscript and Lai Man Adams for technical expertise in crystallization.

References and notes

1. Cuypers, H. T.; Selten, G.; Quint, W.; Zijlstra, M.; Maandag, E. R.; Boelens, W.; Van Wezenbeek, P.; Melief, C.; Berns, A. *Cell* **1984**, *37*, 141.
2. Qian, K. C.; Studts, J.; Wang, L.; Barringer, K.; Kronkaitis, A.; Peng, C.; Baptiste, A.; LaFrance, R.; Mische, S.; Farmer, B. *Acta Crystallogr., Sect. F* **2005**, *61*, 96.
3. Fox, C. J.; Hammerman, P. S.; Cinalli, R. M.; Master, S. R.; Chodosh, L. A.; Thompson, C. B. *Gene Dev.* **1841**, *2003*, 17.
4. MacDonald, A.; Campbell, D. G.; Toth, R.; McLauchlan, H.; Hastie, C. J.; Arthur, J. S. C. *BMC Cell Biol.* **2006**, *7*, 1.
5. Nawijin, M. C.; Alendar, A.; Berns, A. *Nat. Rev.* **2011**, *11*, 23.
6. Santio, N. M.; Vahakoski, R. L.; Rainio, E.; Sandholm, J. A.; Virtanen, S. S.; Prudhomme, M.; Anizon, F.; Moreau, P.; Koskinen, P. J. *Mol. Cancer* **2010**, *9*, 1.
7. Beharry, Z.; Mahajan, S.; Zemskova, M.; Lin, Y.; Tholanikunnel, B. G.; Xia, Z.; Smith, C. D.; Kraft, A. S. *Proc. Natl. Acad. Sci. U.S.A.* **2011**, *108*, 528.
8. Shah, N.; Pang, B.; Yeoh, K.; Thorn, S.; Chen, C. S.; Lilly, M. B.; Salto-Tellez, M. *Eur. J. Cancer* **2008**, *44*, 2144.
9. Haddach, M.;Michauz, J.; Schwaebe, M. K.; Pierre, F.; O'Brien, S. E.; Borsan, C.; Tran, J.; Raffaele, N.; Ravula, S.; Drygin, D.; Siddiqui-Jain, A.; Darjania, L.; Stansfield, R.; Proffitt, C.; Macalino, D.; Streiner, N.; Bliesath, J.; Omori, M.; Whitten, J. P.; Anderes, K.; Rice, W. G.; Ryckman, D. M. *Med. Chem. Lett.* **2011**, Ahead of Print.
10. Nishiguchi, G. A.; Atallah, G.; Bellamacina, C.; Burger, M. T.; Ding, Y.; Feucht, P. H.; Garcia, P. D.; Han, W.; Klivansky, L.; Lindvall, M. *Bioorg. Med. Chem. Lett.* **2011**, *21*, 6366.
11. Pierre, F.; Stefan, E.; Nedellec, A.; Chevrel, M.; Regan, C. F.; Siddiqui-Jain, A.; Macalino, D.; Streiner, N.; Drygin, D.; Haddach, M.; O'Brien, S. E.; Anderes, K.; Ryckman, D. M. *Bioorg. Med. Chem. Lett.* **2011**, *21*, 6687.
12. Tao, Z.; Hasvold, L. A.; Leverson, J. D.; Han, E. K.; Guan, R.; Johnson, E. F.; Stoll, V. S.; Stewart, K. D.; Stamper, G.; Soni, N.; Bouska, J. J.; Luo, Y.; Sowin, T. J.; Lin, N.; Giranda, V. S.; Rosenberg, S. H.; Penning, T. D. *J. Med. Chem.* **2009**, *52*, 6621.
13. Akue-Gedu, R.; Nauton, L.; Thery, V.; Bain, J.; Cohen, P.; Anizon, F.; Moreau, P. *Bioorg. Med. Chem. Lett.* **2010**, *18*, 6865.
14. Lopez-Ramos, M.; Prudent, R.; Moucadel, V.; Sautel, C. F.; Barette, C.; Lafanechere, L.; Mouawad, L.; Grierson, D.; Schmidt, F.; Florent, J.; Filippakopoulos, P.; Bullock, A. N.; Knapp, S.; Reiser, J.; Cochet, C. *FASEB J.* **2010**, *24*, 3171.
15. Grey, R.; Pierce, A. C.; Bemis, G. W.; Jacobs, M. D.; Moody, C. S.; Jajoo, R.; Mohal, N.; Green, J. *Bioorg. Med. Chem. Lett.* **2009**, *19*, 3019.
16. Sliman, F.; Blairvacq, M.; Durieu, E.; Meijer, L.; Rodrigo, J.; Desmaele, D. *Bioorg. Med. Chem. Lett.* **2010**, *20*, 2801.
17. Qian, K.; Wang, L.; Cywin, C. L.; Farmer, B. T.; Hickey, E.; Homon, C.; Jakes, S.; Kashem, M. A.; Lee, G.; Leonard, S.; Li, J.; Magboo, R.; Wang, M.; Pack, E.; Peng, C.; Prokopowicz, A.; Welzel, M.; Wolak, J.; Morwick, T. *J. Med. Chem.* **1814**, *2009*, 52.
18. Tong, Y.; Syewart, K. D.; Thomas, S.; Przytulinska, M.; Johnson, E. F.; Klinghofer, V.; Leverson, J.; McCall, O.; Soni, N. B.; Luo, Y.; Lin, N.; Sowin, T. J.; Giranda, V. L.; Penning, T. D. *Bioorg. Med. Chem. Lett.* **2008**, *18*, 5206.
19. Pierce, A. C.; Jacobs, M.; Stuver-Moody, C. *J. Med. Chem.* **1972**, *2008*, 51.
20. Cheney, I. W.; Yan, S.; Appleby, T.; Walker, H.; Vo, T.; Yao, N.; Hamatake, R.; Hong, Z.; Wu, J. Z. *Bioorg. Med. Chem. Lett.* **2007**, *17*, 1679.
21. Holder, S.; Zemskova, M.; Zhang, C.; Tabrizizad, M.; Bremer, R.; Neidigh, J. W.; Lilly, M. B. *Mol. Cancer Ther.* **2007**, *6*, 163.
22. Pogacic, V.; Bullock, A. N.; Fedorov, O.; Filippakopoulos, P.; Gasser, C.; Biondi, A.; Meyer-Monard, S.; Knapp, S.; Schwaller, J. *Cancer Res.* **2007**, *67*, 6916.
23. Pastor, J.; Oyarzabal, J.; Saluste, G.; Alvarez, R. M.; Rivero, V.; Ramos, F.; Cendón, E.; Blanco-Aparicio, C.; Ajenjo, N.; Cebria, A.; Albarrán, M. I.; Cebrián, D.; Corrionero, A.; Fominaya, J.; Montoya, G. Mazzorana; M *Bioorg. Med. Chem. Lett.* **2012**, *22*, 1591.
24. Bullock, A. N.; Debreczeni, J. E.; Fedorov, O. Y.; Nelson, A.; Marsden, B. D.; Knapp, S. *J. Med. Chem.* **2005**, *48*, 7604.
25. Qian, K. C.; Wang, L.; Hickey, E. R.; Studts, J.; Barringer, K.; Peng, C.; Kronkaitis, A.; Li, J.; White, A.; Mische, S.; Farmer, B. *J. Biol. Chem.* **2005**, *280*, 6130.

26. Jacobs, M. D.; Black, J.; Futer, O.; Swenson, L.; Hare, B.; Fleming, M.; Saxena, K. *J. Biol. Chem.* **2005**, *280*, 13728.
27. Data generated in house.
28. Detailed experimentals for this manuscript are found in the following patent: Brown, S.D.; Du, H.; Franzini, M.; Galan, A.A.; Huang, P.; Kearney, P.; Kim, M.H.; Koltun, E.S.; Richards, S.J.; Tsuhako, A.L.; Zaharia, C.A. WO 2009086264 A1 2009.
29. Human PIM1 (E32-D292), PIM2 (E26-A306) and PIM3 (K30-L326) were expressed as N-terminally His-tagged proteins in *E. coli* and purified using nickel affinity chromatography. Human CK2 α isoform A (amino acids: R8–R333) and full-length β subunits were expressed separately as N-terminally MBP-tagged proteins in *E. coli* and purified using amylose Sepharose chromatography. The purified subunits were reconstituted to form the tetrameric $\alpha_2\beta_2$ CK2 holoenzyme. Protein concentration was determined by the Bradford assay and identification was confirmed by trypsin digestion and mass spectrometry. Kinase activity and compound inhibition were determined using the luciferase-luciferin-coupled chemiluminescence assay and measured as the percentage of ATP utilized following the kinase reaction in a 384-well format as described previously (Ref. 29). The final PIM kinase assay condition was 0.5 μM ATP, 10 μM peptide substrate (AKRRRLSA), 20 mM Hepes pH 7.4, 10 mM $MgCl_2$, 0.03% Triton, and 1 mM DTT. The kinase concentrations were 2.4 nM for PIM1, 4 nM for both PIM2 and PIM3. The final CK2 kinase assay condition was 4 nM CK2 holoenzyme, 2 μM ATP, 2 μM casein, 20 mM Hepes pH 7.5 10 mM $MgCl_2$, 0.03% Triton, 1 mM DTT and 0.1 mM $NaVO_3$. All kinase reactions were incubated at room temperature for 1–2 h.
30. Munagala, N.; Nguyen, S.; Lam, W.; Lee, J.; Joly, A.; McMillan, K.; Zhang, W. *Assay Drug Dev. Technol.* **2007**, *5*, 65.
31. BAD Phosphorylation ELISA Analysis: HEL92.1.7 cells (AML) stably transfected with wildtype BAD (clone 2B8) were seeded at 1.5×10^5 cells/well onto 96-well plates (Costar, 3628), in serum-free RPMI (ATCC) containing 1% penicillin–streptomycin (Cellgro). Dimethyl sulfoxide (DMSO, ATCC) or serial dilutions of compounds in fresh serum-free medium were added to the cells and incubated for 1 h at 37 °C, 5% CO_2. Medium was removed and the cells were lysed with 100 μL cold lysis buffer (0.1% Triton X-100 lysis buffer). Protein lysates (20 μL and 20 μL) for detection of phosphorylated BAD and total BAD, respectively, were incubated overnight at 4 °C in 96-well high-binding plates (Pierce, 15042), coated with mouse anti-FLAG M2 (1 μg/mL, Sigma Aldrich, F3165). Immuno-complexes were washed three times with TBST (25 mM Tris–HCl, pH 7.2, 150 mM NaCl, 0.1% Tween-20) and incubated for 3 h in TBST buffer containing either rabbit anti-pBAD (Ser116) (1:1,500, Cell Signaling) or total BAD (1:1,000, Epitomics,) antibodies. Immuno-complexes were washed and incubated for 1 h in TBST containing HRP-conjugated goat anti-rabbit IgG (1:10,000, Pierce). Immuno-complexes were then washed, followed by the addition of a luminol-based substrate solution (Pierce, 37069) before measurements were taken in a Victor Wallac V multiwavelength measurement reader (Perkin Elmer). The percentage inhibition of BAD phosphorylation was normalized to total BAD and the IC_{50} values were calculated from six different compound concentrations.